53 29 35 CONFIDENTIAL

Copy No. 121

RM No. A7A15

A 7 A 15

9262

TECH LIBRARY KAFB, NM
0142991

RESEARCH MEMORANDUM

FLIGHT-TEST MEASUREMENTS OF AILERON CONTROL SURFACE BEHAVIOUR AT SUPERCRITICAL MACH NUMBERS

By

Harvey H. Brown,
George A. Rathert, Jr., and
Lawrence A. Clousing

Ames Aeronautical Laboratory
Moffett Field, Calif.

CLASSIFIED DOCUMENT

This document contains classified information affecting the National Defense of the United States within the meaning of the Espionage Act, [illegible], its transmission or the revelation of its contents in any manner to an unauthorized person is prohibited by law.

Information classified may be imparted only to persons in the military and naval services of the United States, appropriate civilian officers and employees of the Federal Government who have a legitimate interest therein, and to United States citizens of known loyalty and discretion who of necessity must be informed thereof.

NATIONAL ADVISORY COMMITTEE
FOR AERONAUTICS

WASHINGTON

April 23, 1947

CONFIDENTIAL

319.98/13

TECH LIBRARY KAFB, NM
0142991

NATIONAL ADVISORY COMMITTEE FOR AERONAUTICS

RESEARCH MEMORANDUM

FLIGHT-TEST MEASUREMENTS OF AILERON CONTROL-SURFACE BEHAVIOUR AT SUPERCRITICAL MACH NUMBERS

By Harvey H. Brown,
George A. Rathert, Jr.,
and Lawrence A. Clousing.

SUMMARY

The behaviour at supercritical Mach numbers of the ailerons of a jet-propelled fighter has been measured up to 0.866 Mach number. The considerable amount of aileron upfloat occurring at these Mach numbers was found to be due to a large loss in pressure recovery on the upper surface aft of the shock wave which caused very large increases in the aileron hinge moments. Data obtained from pressure-distribution measurements are presented to show the very critical effect of Mach number on the magnitude of these hinge moments.

Aileron oscillations were also encountered, ranging in severity from a spasmodic low-amplitude "buzz" to a motion so violent the aileron was deformed. The comparatively mild buzz should be considered a preliminary warning of the appearance of the more severe and dangerous oscillations. The flight condition boundary defining the first appearance of the buzz is presented in terms of Mach number and both the airplane lift coefficient and the average section normal-force coefficient over the aileron. This flight-test boundary is in excellent agreement with wind-tunnel tests of a partial-span full-scale wing with the aileron free. Typical aileron angle and pressure-distribution records are also presented to illustrate some of the characteristics of the oscillations.

INTRODUCTION

In the past few years, experience during high-speed flight has indicated serious changes in the behaviour of the aileron control surfaces at speeds above the critical Mach numbers of the airfoil sections now in use. Such changes have been evidenced by large amounts of aileron upfloat, indicating large changes in the magnitude of the air loads and hinge moments, and the appearance of aileron oscillations.

In the course of wing pressure-distribution measurements and various other tests of a turbojet-propelled fighter examples of this behaviour at supercritical Mach numbers have been encountered several times. During the highest speed dive, in which a Mach number of 0.866 was reached, the severity of the aileron oscillations increased quite rapidly and the motion became so violent that one aileron was deformed. So far as is known, this is the only time the more violent and dangerous oscillation has been encountered in flight.

This report presents a summary of all the data on aileron behaviour at supercritical Mach number which have been obtained incidental to these scheduled tests.

DESCRIPTION OF THE AIRPLANE AND THE INSTRUMENTATION

The tests were conducted on the turbojet-propelled fighter airplane shown in the three-view drawing. (See fig. 1.) Figures 2 and 3 are side-view and plan-form photographs, respectively, of the airplane as instrumented for flight tests.

The dimensions of the wing and aileron are listed in table I. Table II contains the ordinates for the theoretical wing contour (NACA 651-213 (a = 0.5)). The deviations of the actual wing sections from the theoretical contour are presented in figure 4 for each of the four pressure-distribution-orifice stations.

The aileron control system of this type of airplane was unusually rigid as compared with other present-day fighter airplanes and employed a power boost in operating the ailerons. The ailerons were equipped with piano-type hinges located on the upper surface of the wing and were approximately statically and dynamically mass-balanced but had no aerodynamic balance. Throughout the test program the aileron cable tension was rigged at 300 pounds at 70° F.

Standard NACA instruments were used to record the aileron angle, normal acceleration factor, pressure altitude, indicated airspeed, and wing-pressure distribution.

ACCURACY OF RESULTS

The static pressures used in computing the values of Mach number and pressure coefficient were obtained by correcting the static pressure at the free-swivelling airspeed head mounted on the right-wing tip (fig. 2) for position error as determined from a low-altitude flight calibration. In addition, the error inherent in the airspeed head itself due to compressibility was determined from a calibration made in the Ames 16-foot high-speed wind tunnel and corrections were made. The airspeed recorder, altimeter, and all other pressure cells were calibrated at several temperatures to permit removal of temperature effects from the data. The accuracy of the data is as follows:

$$M = \pm 0.005$$
$$P = \pm 10/q$$
$$\delta a = \pm 0.2^{\circ}$$

The symbols used throughout the report are presented in the appendix.

RESULTS AND DISCUSSION

Aileron Upfloat

The effect of Mach number on the upfloating angle of the ailerons is shown for various values of airplane lift coefficient in figure 5. The line curves were obtained from measurements of the right aileron position only, during a series of very high-speed dives. Subsequent measurements of the mean deflection of both ailerons, indicated in figure 5 by symbols, substantiated the trends of the data obtained from the right aileron alone.

Since the aileron control system was quite rigid, the large upfloating angles obtained indicated that very large hinge moments were being encountered. The magnitudes of the hinge moments at zero aileron angle were determined by using the pressure distributions over the aft 25 percent of the wing inboard of the ailerons (fig. 1) to compute the moment coefficients about the 75-percent-chord line. These data are presented in figure 6 and show that for zero aileron deflection

the hinge moments become extremely large at supercritical Mach numbers. It is further apparent that in this speed range the hinge moments are a sensitive function of Mach number.

The reason for these large hinge moments is illustrated by figure 7. In this figure a chordwise pressure distribution at a subcritical Mach number is contrasted with another at the same airplane lift coefficient but at a Mach number considerably above the critical. In comparison, the supercritical Mach number distribution shows a very large loss in pressure recovery aft of the shock wave which is responsible for the increase in hinge moment. This large loss in pressure recovery is presumably due to shock induced separation on the upper surface.

The effect of aileron deflection on the critical Mach number of the theoretical airfoil section, calculated by the method of reference 1 for the range of upfloating angles encountered, is presented in figure 8. A few experimental values from the flight-test pressure distributions are included. A comparison indicates the flight-test critical Mach number to be from 0.015 to 0.025 lower than the theoretical.

Aileron Oscillations

A low-amplitude aileron oscillation known as "buzz" was encountered several times during the flight tests. This buzz was spasmodic when first encountered but as the speed increased became a sustained oscillation with a frequency of approximately 28 cycles per second and a range of movement of about 2°. Typical aileron-angle records during buzz at various Mach numbers are reproduced in figure 9. Figure 10(a) is a photograph of the left aileron taken during the buzz, showing the blurred image of the trailing edge. The angle between the converging images of the upper edge of the black stripe across the aileron indicates the small amplitude of the motion.

At a Mach number of about 0.85 during a high-speed dive the buzz developed into a much higher amplitude oscillation of sufficient violence to cause the trailing edge of the left aileron to buckle. Figure 11 is a time history of a portion of this dive and pull-out showing the record of the right aileron position. The records indicated that the aileron oscillated about an up-position over a range of about 6°, but the frequency could not be determined. The photograph of the left aileron during the flutter (fig. 10(b)) shows the considerable increase in the angle formed by the images of the edge of the black stripe. The double image of the star insignia indicates the amount of general buffeting accompanying the aileron oscillations.

Figure 12 is a photograph of the aileron taken after the flight to show the buckle in the trailing edge caused by the flutter.

A flight-test boundary defining the first appearance of spasmodic buzz in terms of Mach number and airplane lift coefficient is presented as the solid line in figure 13. Corresponding values of the average section normal-force coefficient of the wing section through the aileron are spotted on the curve for convenient reference.

At higher Mach numbers the buzz became a steady and sustained motion, as indicated on figure 13 by the square symbols. Further increases in Mach number resulted in transition to the more violent and severe flutter indicated by the circles. It is probable, however, that the location of this transition can be shifted by changes in the amount of cable tension or aileron restraint. For this reason the specific increment in Mach number indicated in figure 13 between the buzz and the more dangerous oscillation should not be interpreted as a generally applicable factor of safety.

Figure 14 is a boundary for the first appearance of aileron oscillations which is expressed in terms of the average section normal-force coefficient of the wing section through the aileron rather than the airplane lift coefficient. The flight-test boundary falls only 0.007 Mach number below the data[1] from tests in the Ames 16-foot high-speed wind tunnel of a partial-span installation of an identical full-scale wing with a free aileron. This close agreement between tests conducted with high cable tension and with no restraint at all demonstrates the validity of using the buzz boundary as a signal of possible dangerous flutter at some higher Mach number, depending upon the amount of restraint and damping in the aileron control system.

The section critical Mach numbers, determined both from flight tests and from theory, are also presented in figure 14 to show that the buzz actually occurs at a practically constant increment of Mach number above the section critical Mach number, regardless of the value of the section normal-force coefficient or the airplane lift coefficient.

The cause of the aileron oscillations has been determined from the wind-tunnel tests of the partial-span installations of a full-scale wing. Shadowgraph pictures taken during these

[1]Unpublished data on file at this laboratory

tests demonstrate that there is a coupling between the aileron motion and shock-induced separation originating forward of the aileron. In view of this explanation an examination of the pressure measurements in the region of the aileron, obtained during the oscillations, is of interest.

Figures 15 and 16 present pressure distributions both for a wing station over the aileron (station 152) and inboard of the aileron (station 105.25) during the buzz at M = 0.850 and the more violent oscillations or flutter at M = 0.866, respectively. The pressure-distribution records for the orifices on the aileron indicate severe flow separation on the upper surface of the wing during the violent flutter. During the buzz, pressures on both the upper and lower surfaces of the aileron remained steady, largely due to the small amplitude of the motion. During the more violent flutter, however, as noted in figure 16, the pressures on the lower surface showed the extreme fluctuations which would be expected with a rapid motion over a range of 6°. The upper-surface pressures, however, were quite steady, which is presumed to indicate that the orifices were always in a region of severe flow separation. Two pressure-cell records from station 152 which are typical of all pressure records on the aileron are presented in figure 17 and illustrate this difference in behaviour.

Flight-test measurements of the chordwise location of the shock at the supercritical Mach numbers at which aileron oscillations occurred (0.80 to 0.86) are shown in figure 18 for both the upper and lower surfaces. The location of the shock was defined as the chordwise location at which a sharp break in the pressure distribution occurred. It is interesting to note that in this Mach number range the location of the upper-surface shock has stopped moving aft with increasing Mach number and has become fixed; whereas the lower surface shock is still moving aft. These results indicate the wide variety in flow conditions under which oscillations of the aileron may occur.

CONCLUSIONS

An analysis of the behaviour at supercritical Mach numbers of the ailerons of a typical turbojet-propelled fighter has led to the following:

1. The considerable loss in pressure recovery on the upper surface aft of the shock wave produced large increases in the aileron air loads and hinge moments, resulting in large aileron upfloating angles. The increases in loading imposed on the aileron structure and the control system warrant serious consideration in the design of high-speed aircraft.

2. The first appearance of aileron oscillations in flight was established in terms of a boundary defined by the Mach number and both the airplane lift coefficient and the average sectional normal-force coefficient of the wing section through the aileron. The oscillations always appeared at a practically constant increment of Mach number above the section critical Mach number.

3. The severity of the aileron oscillations increased rapidly to the highest test Mach number, and the motion became so violent one aileron was deformed. Good agreement between buzz boundaries established by flight tests of a restrained aileron and wind-tunnel tests of a free aileron indicated that the buzz boundary is a useful signal of the possible appearance of more violent and dangerous oscillations at some higher Mach number, depending on the amount of restraint and damping in the aileron control system.

Ames Aeronautical Laboratory,
National Advisory Committee for Aeronautics,
Moffett Field, Calif.

Harvey H. Brown
Harvey H. Brown,
Aeronautical Engineer.

George A. Rathert Jr.
George A. Rathert, Jr.,
Aeronautical Engineer.

Lawrence A. Clousing
Lawrence A. Clousing,
Engineer-Test Pilot.

Approved:

John F. Parsons
John F. Parsons,
Aeronautical Engineer.

APPENDIX

SYMBOLS

A_Z airplane normal acceleration factor (Z/W)

c wing section chord, ft

c_h section hinge-moment coefficient

$$16\int_{0.75}^{1.00}(P_U-P_L)\left(\frac{x}{c}-0.75\right)d\left(\frac{x}{c}\right)$$

C_L airplane lift coefficient, computed by the formula A_ZW/qS

c_n section normal-force coefficient

$$\int_{0}^{1.0}(P_L-P_U)\ d\left(\frac{x}{c}\right)$$

M Mach number, ratio of airspeed to speed of sound

P pressure coefficient $\left(\frac{p-p_o}{q}\right)$

P_U pressure coefficient on upper surface

P_L pressure coefficient on lower surface

p static orifice pressure, lb/sq ft

p_o free-stream static pressure, lb/sq ft

q dynamic pressure $(\frac{1}{2}\rho V^2)$, lb/sq ft

S wing area, sq ft

x chordwise location from leading edge, ft

W airplane gross weight, lb

Z aerodynamic normal force on airplane, lb

δ_a aileron control-surface deflection, deg

REFERENCE

1. Heaslet, Max. A., and Pardee, Otway O'D.: Critical Mach Numbers of Thin Airfoil Sections with Plain Flaps. NACA ACR No. 6A30, 1946.

TABLE I.- BASIC DIMENSIONAL DATA OF THE TEST AIRPLANE.	
Wing	
Area, sq ft	237
Span, ft	38.9
Aspect ratio	6.39
Taper ratio	0.364
Mean aerodynamic chord, in.	80.6
Dihedral of trailing edge of wing, deg	3.83
Incidence[1] root chord, deg	1.00
Geometric twist, deg	1.50 washout from root to tip
Root section	NACA 65_1-213 (a=0.5)
Tip section	NACA 65_1-213 (a=0.5)
Percent line, straight	52.0
Aileron	
Area aft of hinge line, sq ft (both sides)	17.14
Fixed surface affected by movable surface, sq ft (both sides)	67.1
Span, ft (one sido)	7.21
Mean aerodynamic chord, ft	1.216
Hinge-line location, percent chord	75.0
Type of aileron	No aerodynamic balance, piano hinge on upper surface, power-boost control system, approximately statically and dynamically mass-balanced
Travel	±20°
Tabs	Trim tab on left aileron

[1]Incidence measured with respect to thrust line.

TABLE II.- ORDINATES OF NACA 65_1-213 (a = 0.5) AIRFOIL
[All stations and ordinates in percent chord]

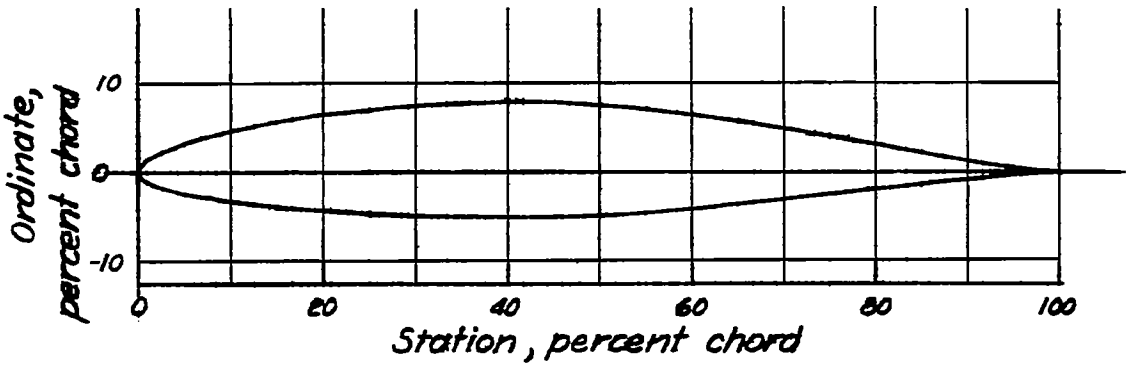

NATIONAL ADVISORY COMMITTEE
FOR AERONAUTICS

Upper surface		Lower surface	
Station	Ordinate	Station	Ordinate
0	0	0	0
.38	1.06	.62	-.92
.62	1.29	.88	-1.10
1.10	1.64	1.40	-1.35
2.34	2.28	2.66	-1.76
4.81	3.26	5.19	-2.38
7.31	4.02	7.69	-2.84
9.80	4.67	10.20	-3.22
14.81	5.71	15.19	-3.82
19.83	6.51	20.17	-4.26
24.86	7.12	25.14	-4.59
29.89	7.56	30.11	-4.82
34.92	7.85	35.08	-4.96
39.96	7.98	40.04	-5.01
45.01	7.94	44.99	-4.95
50.07	7.71	49.93	-4.77
55.11	7.26	54.89	-4.47
60.13	6.63	59.87	-4.07
65.14	5.89	64.86	-3.60
70.13	5.04	69.87	-3.06
75.11	4.14	74.89	-2.49
80.09	3.19	79.91	-1.88
85.06	2.24	84.94	-1.29
90.04	1.33	89.97	-.72
95.01	.53	94.99	-.24
100.00	0	100.00	0

L. E. radius: 1.174. Slope of radius through L. E.: 0.084

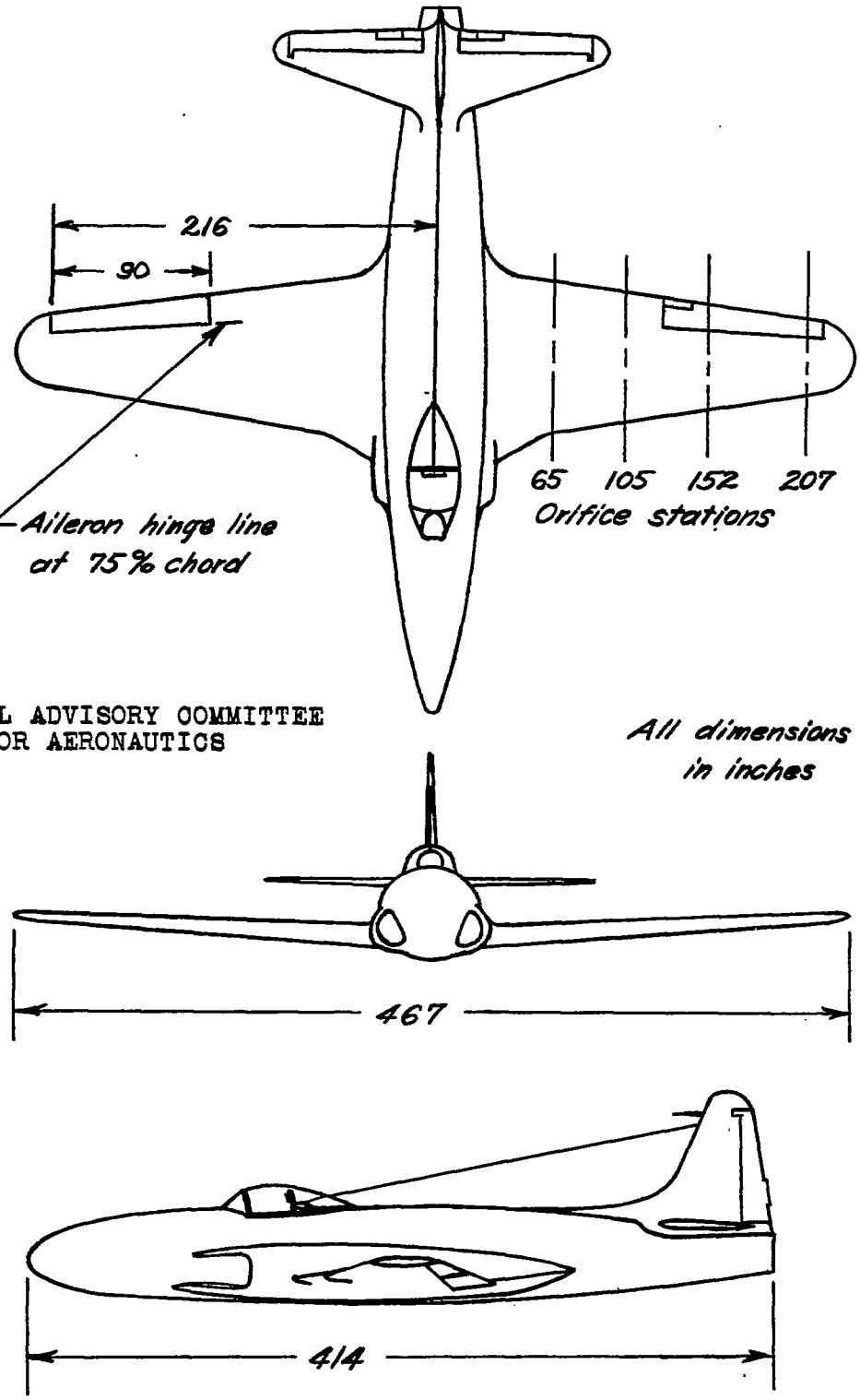

Figure 1. —— Three-view drawing of the test airplane.

CONFIDENTIAL

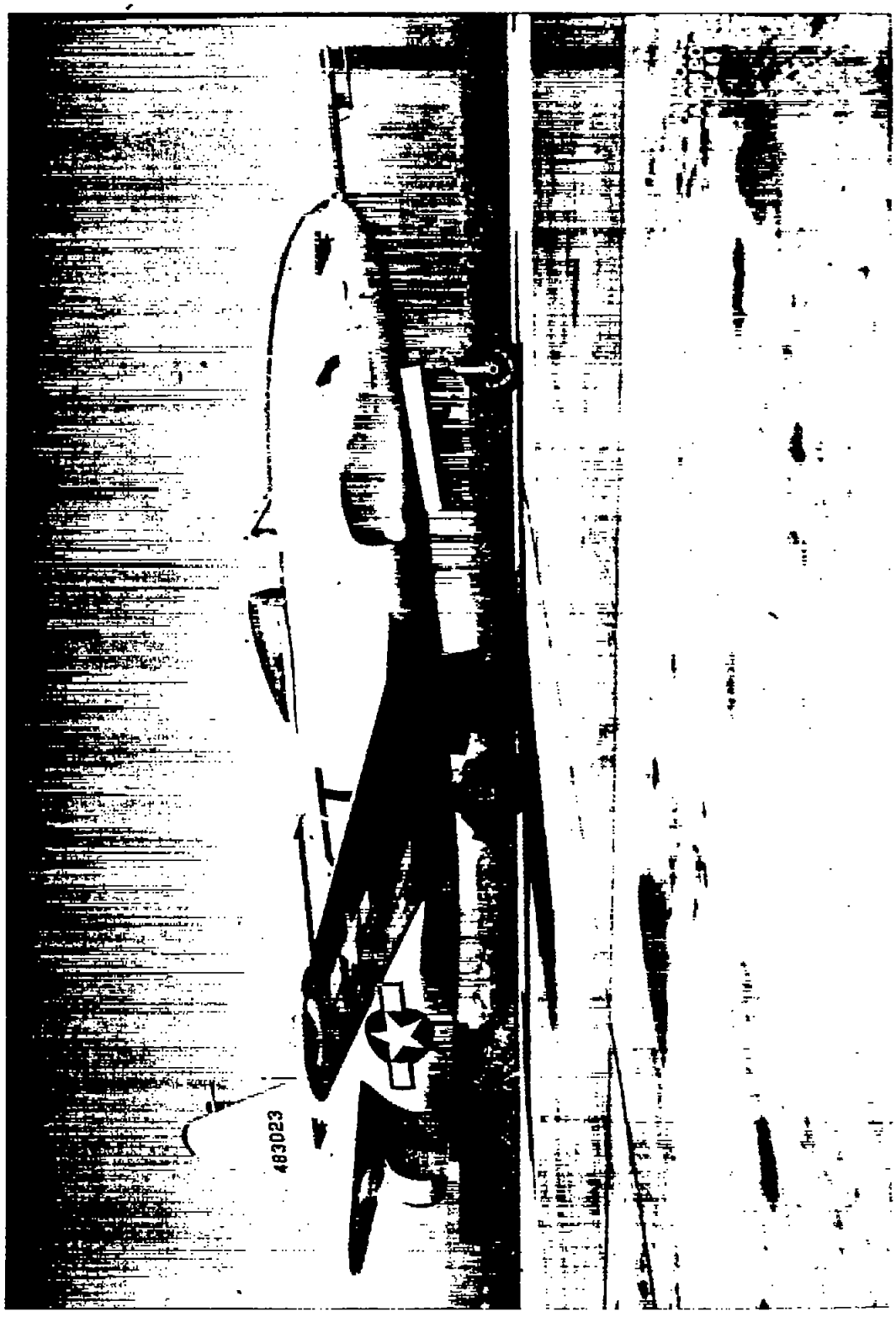

Figure 2.- Side view of the test airplane as instrumented for flight tests.

CONFIDENTIAL

CONFIDENTIAL

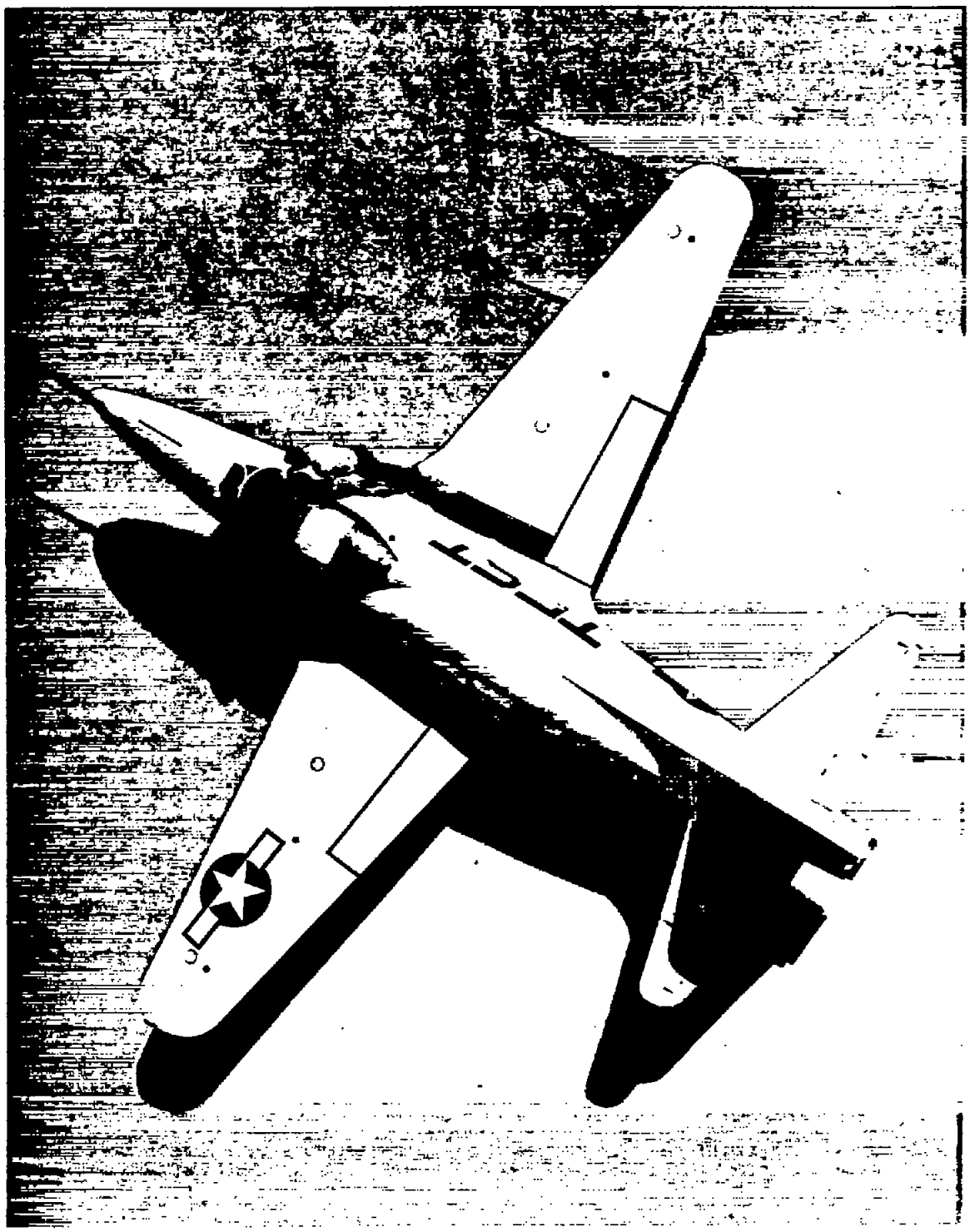

Figure 3.- Plan view of the test airplane as instrumented for flight tests.

CONFIDENTIAL

CONFIDENTIAL

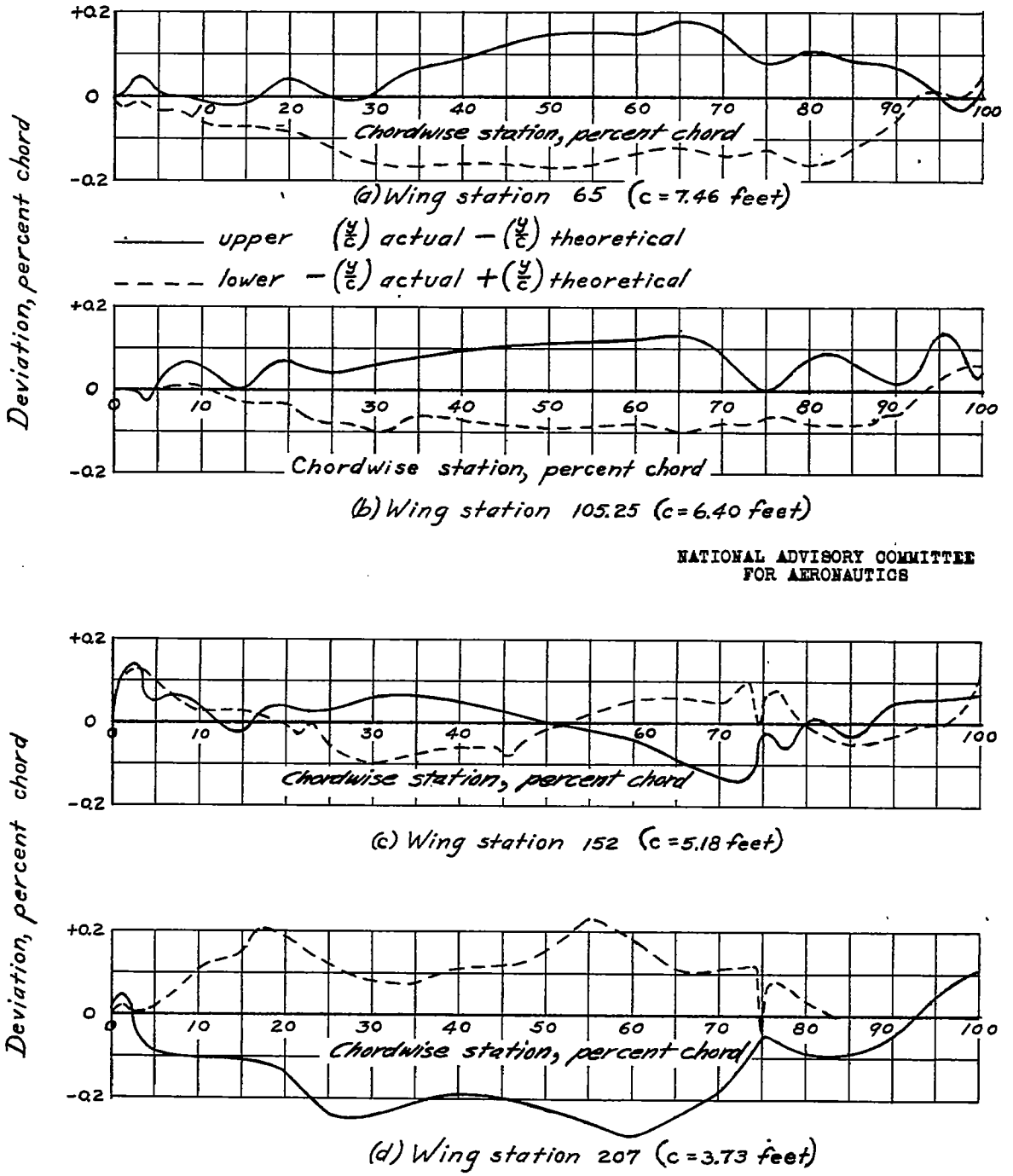

Figure 4. — Deviation in percent chord of actual wing contour from the theoretical airfoil at various spanwise locations.

CONFIDENTIAL

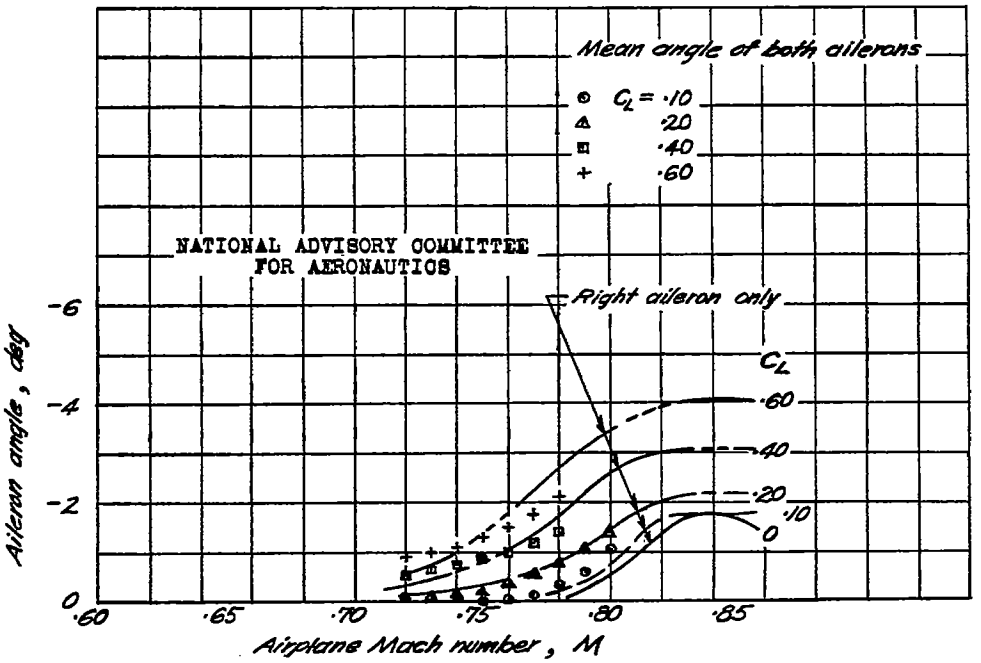

Figure 5. —— Variation of aileron angle with airplane Mach number.

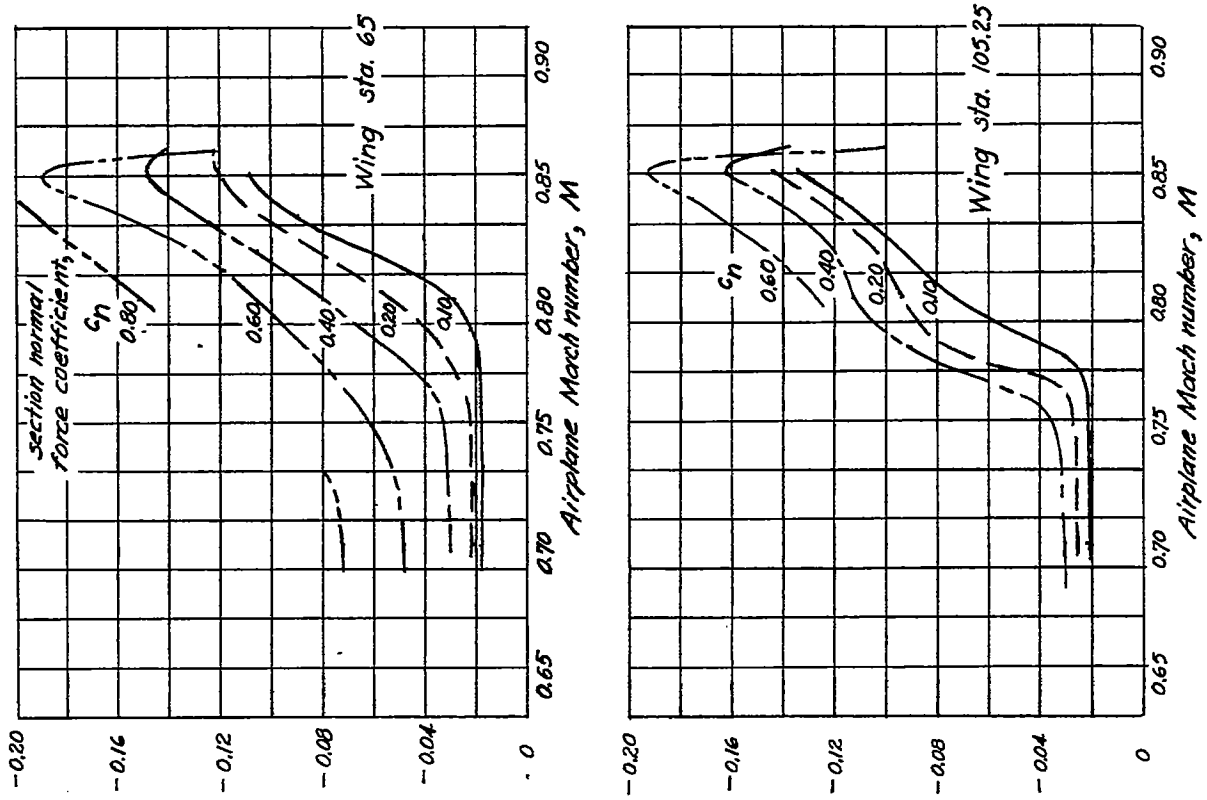

Figure 6. —— Variation of section hinge-moment coefficient with Mach number at various section normal-force coefficients for wing stations inboard of ailerons, $\delta_a = 0$.

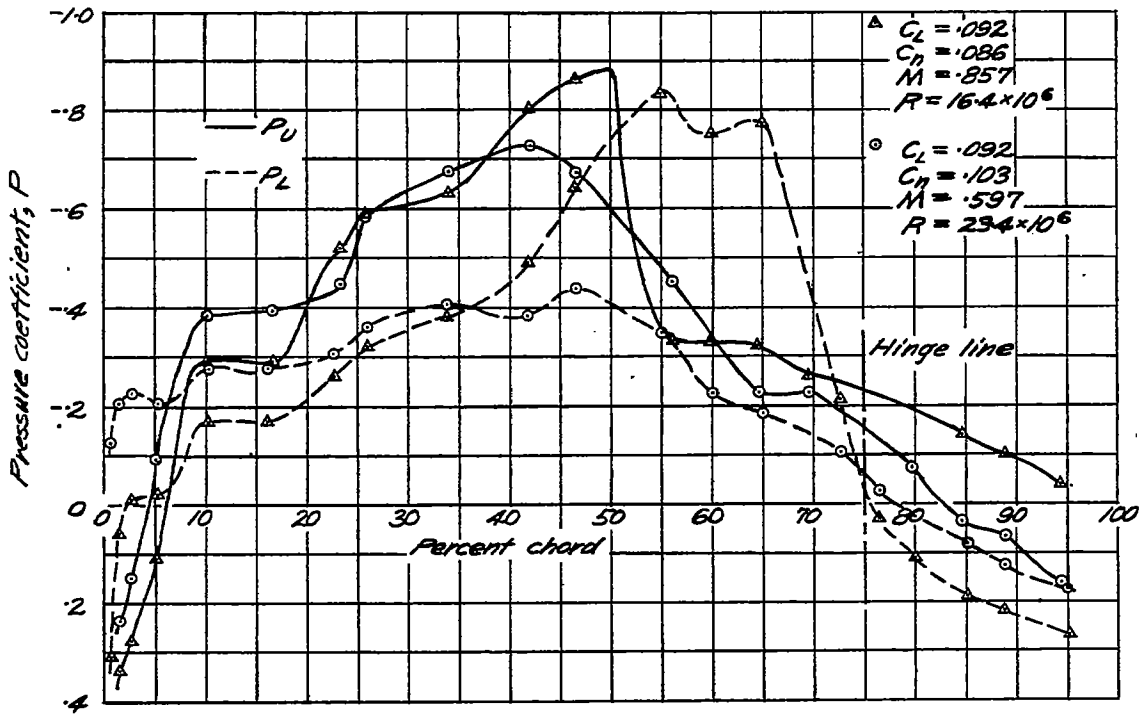

Figure 7. —— Comparison of pressure distributions over wing station 105.25 at different Mach numbers.

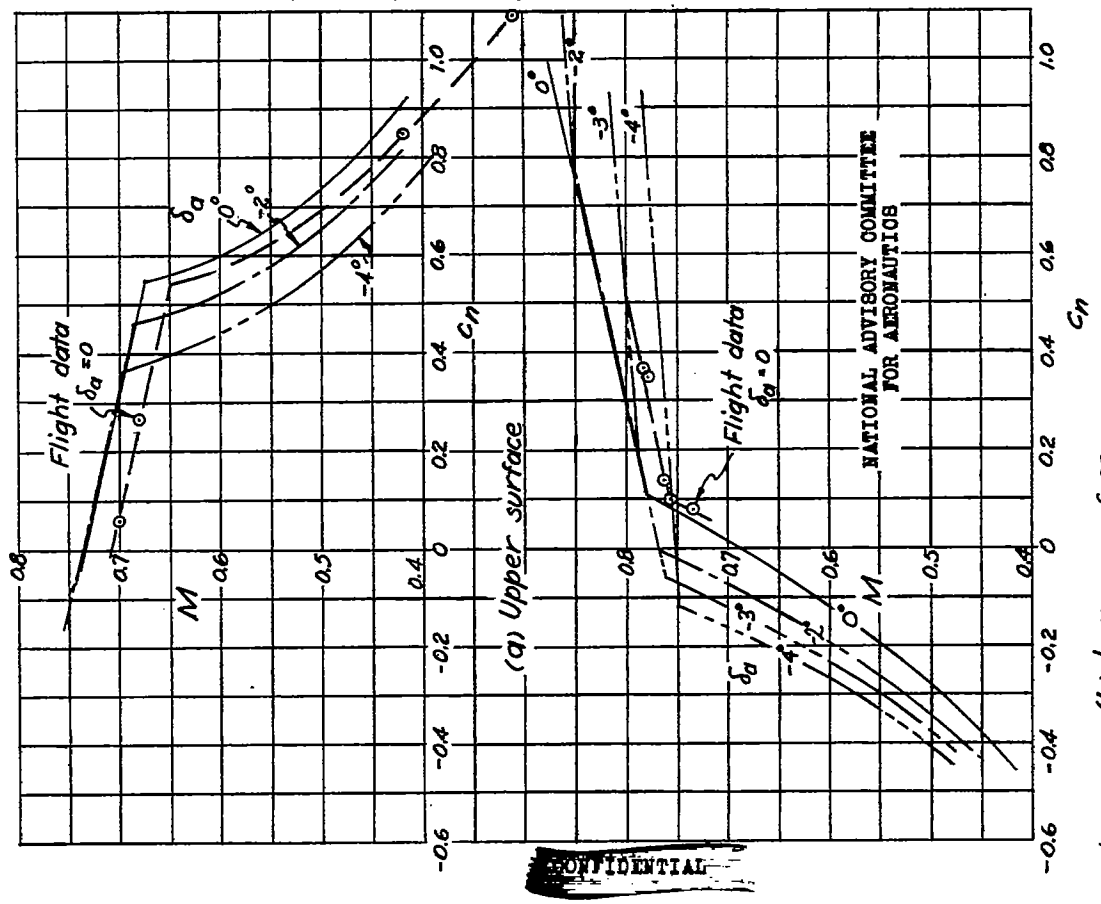

Figure 8. —— Variation of theoretical critical Mach number with normal-force coefficient for the NACA 65,-213 (a=0.5) airfoil and comparison with flight-test data.

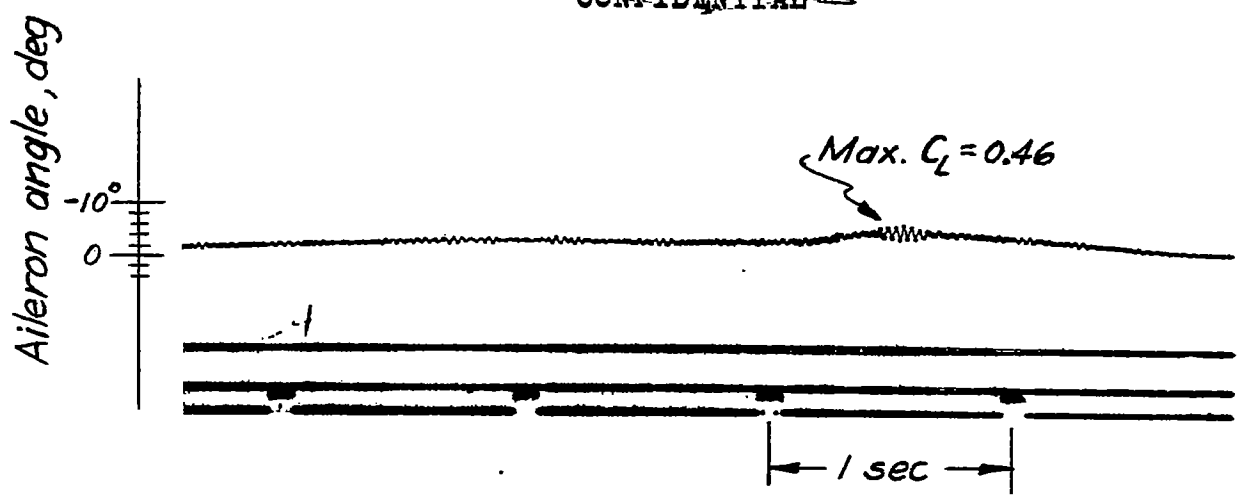

(a) M = 0.80

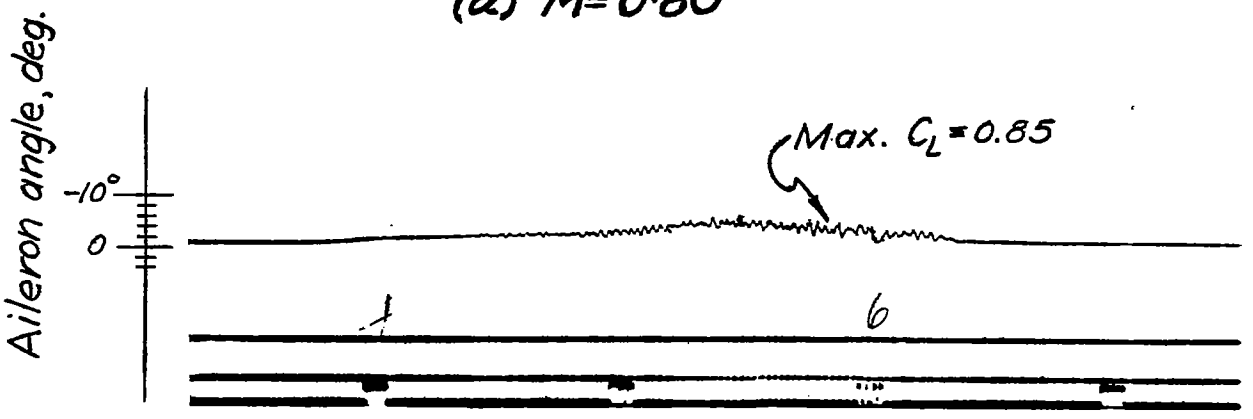

(b) M = 0.77

NATIONAL ADVISORY COMMITTEE
FOR AERONAUTICS

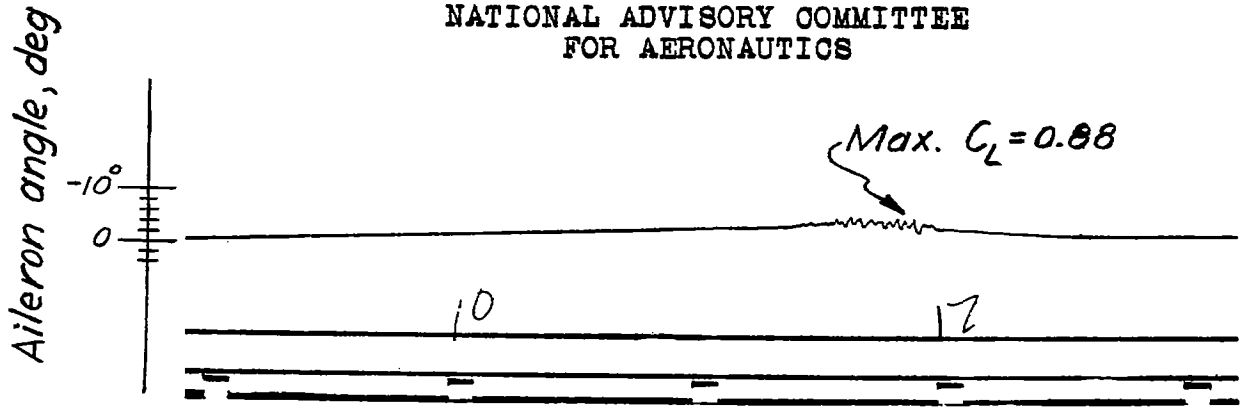

(c) M = 0.70

Figure 9.- Typical records of right aileron position during pull-ups at various Mach numbers showing oscillations.

CONFIDENTIAL

(a) During buzz, $M = 0.826$, $C_L = 0.01$.

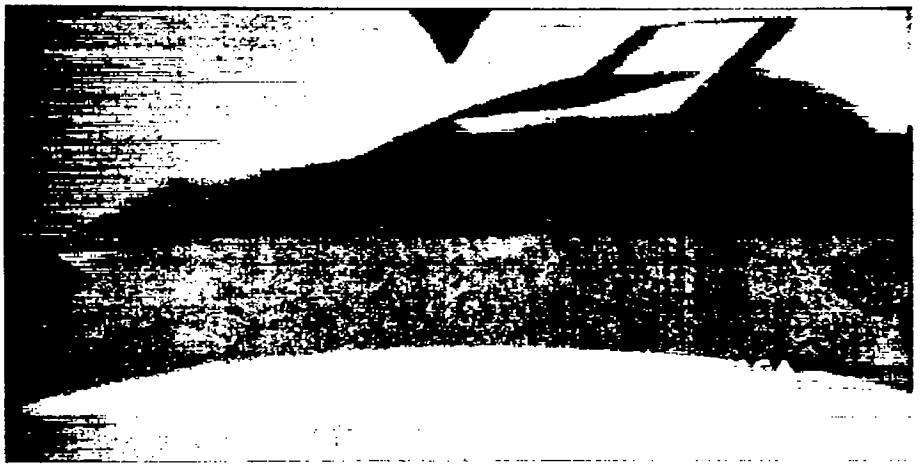

(b) During flutter, $M = 0.865$, $C_L = 0.35$

Figure 10.- Photographs of the left aileron during aileron oscillations.

CONFIDENTIAL

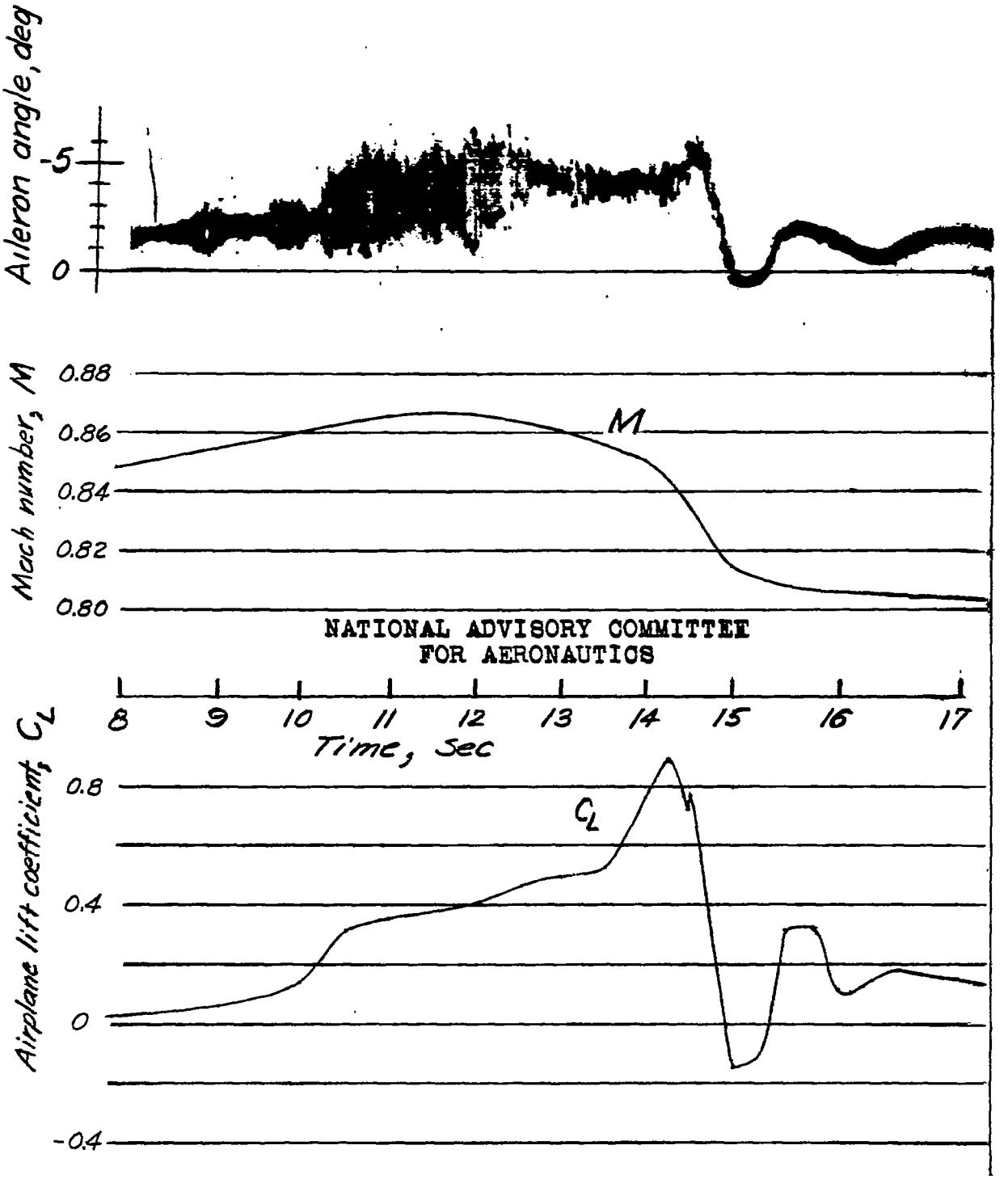

Figure 11.- Records of right aileron upfloat and oscillations during dive recovery at Mach number and airplane lift coefficient shown.

CONFIDENTIAL

CONFIDENTIAL

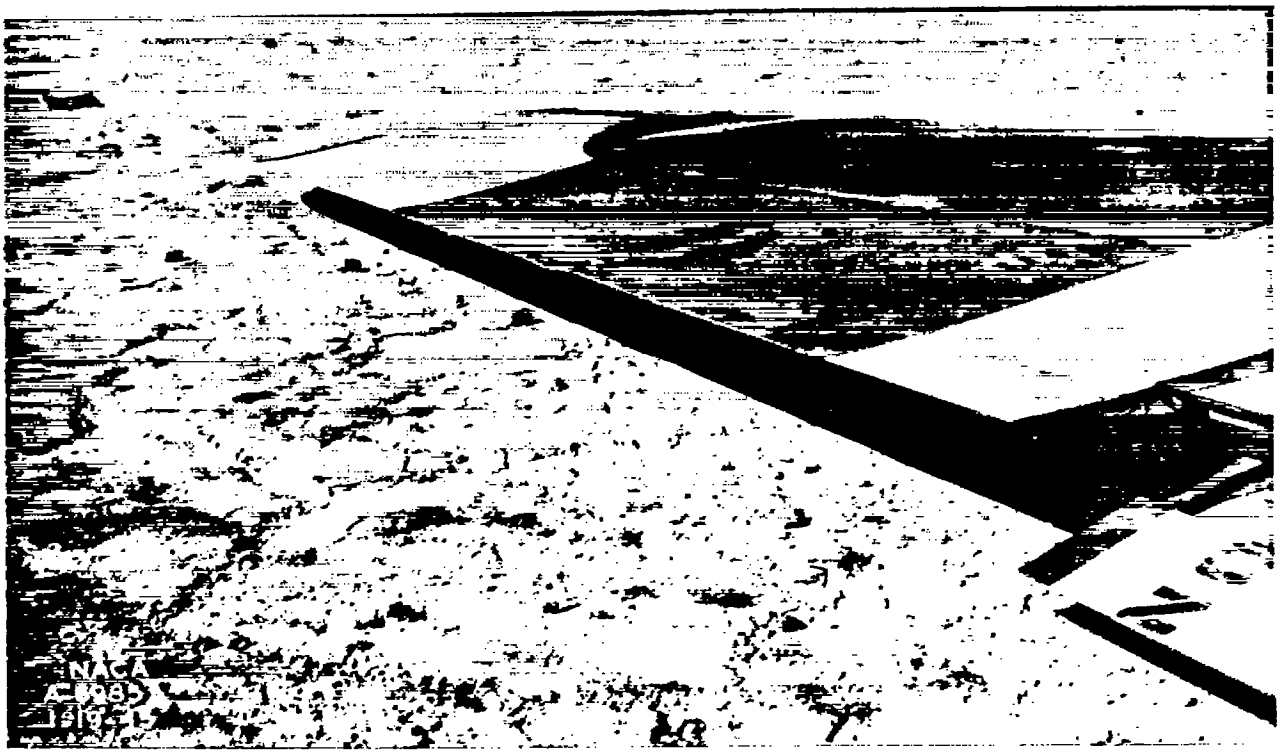

Figure 12.- Photograph of left aileron taken on ground after dive recovery showing buckled trailing edge caused by severe flutter.

CONFIDENTIAL

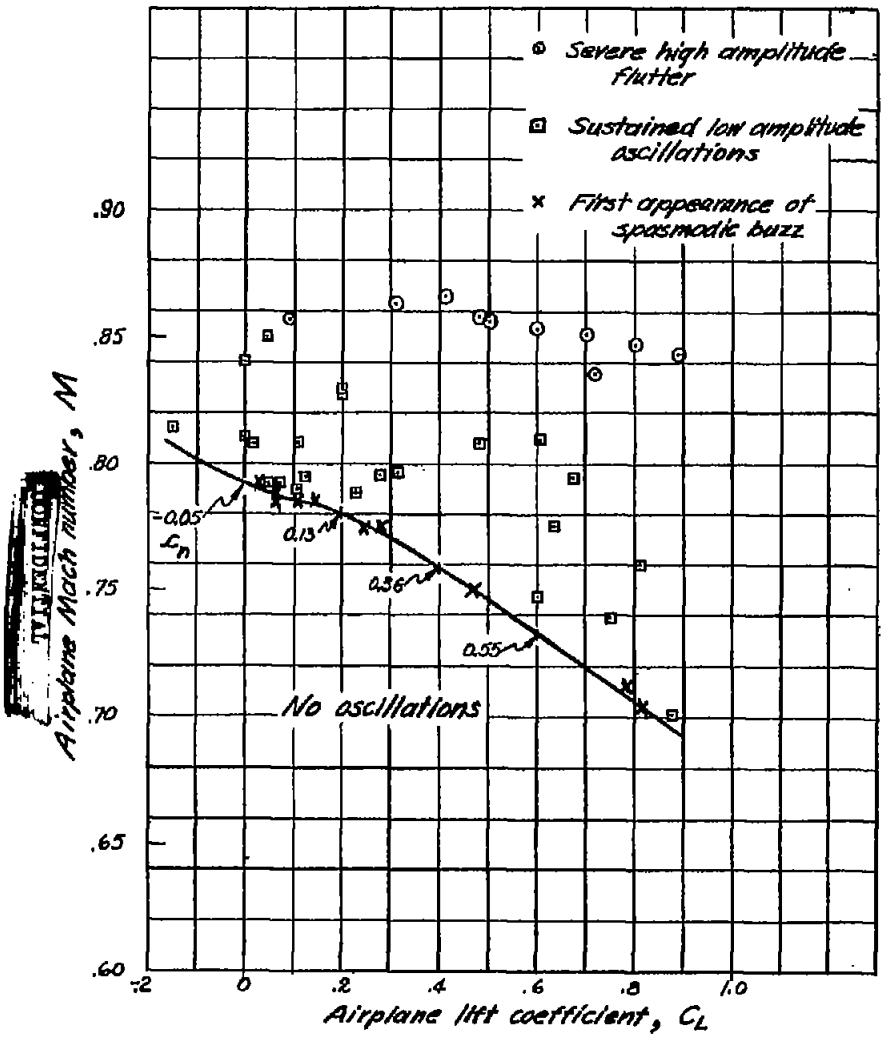

Figure 13 . — The range of Mach number and airplane lift coefficient in which aileron oscillations occurred on the test airplane.

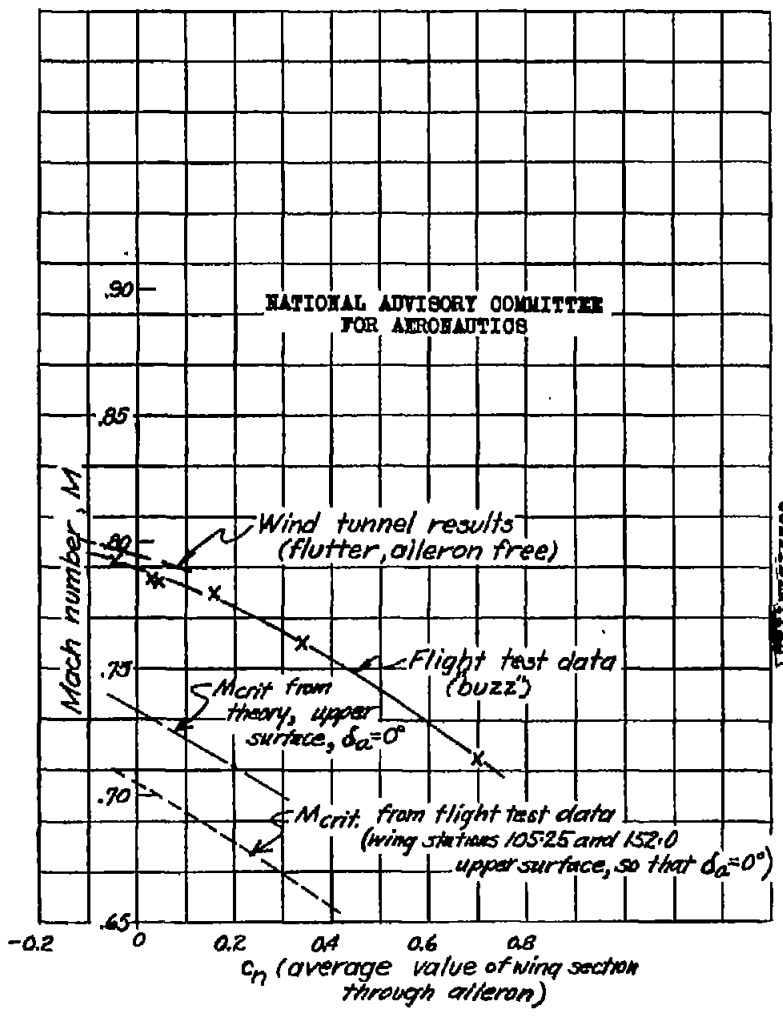

Figure 14.— Variation of Mach number at which aileron oscillations occur with normal-force coefficient.

CONFIDENTIAL

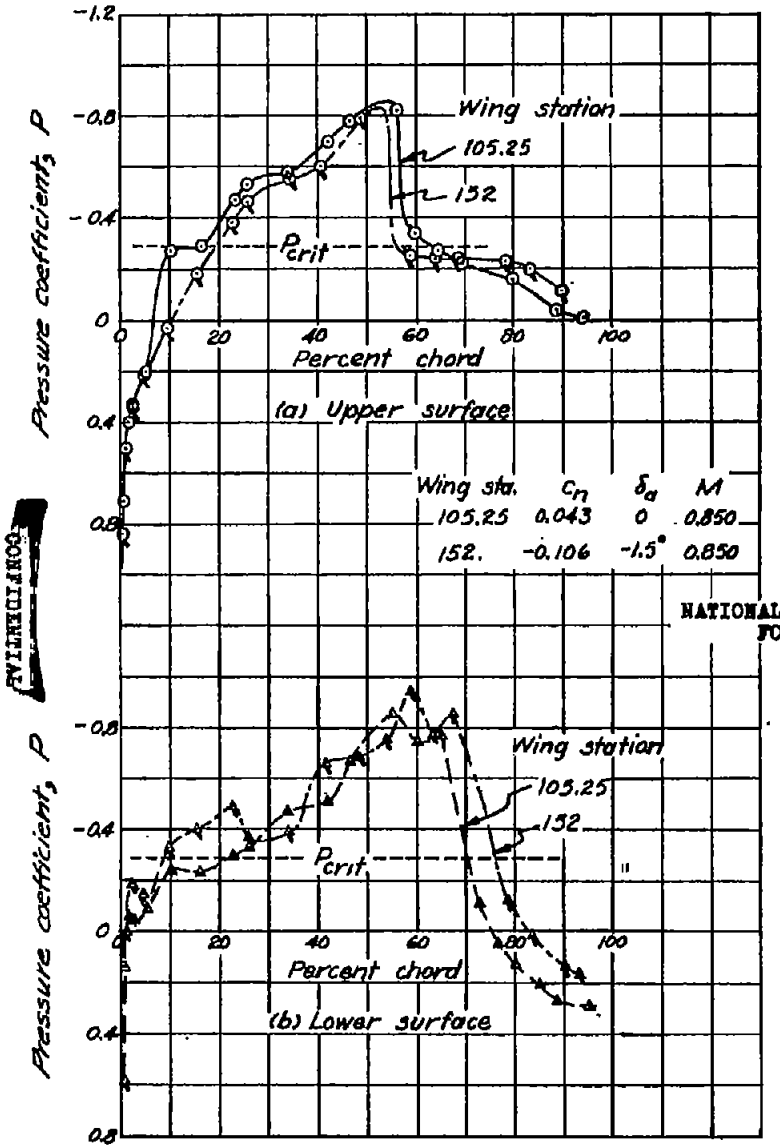

Figure 15. — Comparison between chordwise pressure distributions during buzz at wing stations inboard of and at the aileron.

NATIONAL ADVISORY COMMITTEE FOR AERONAUTICS

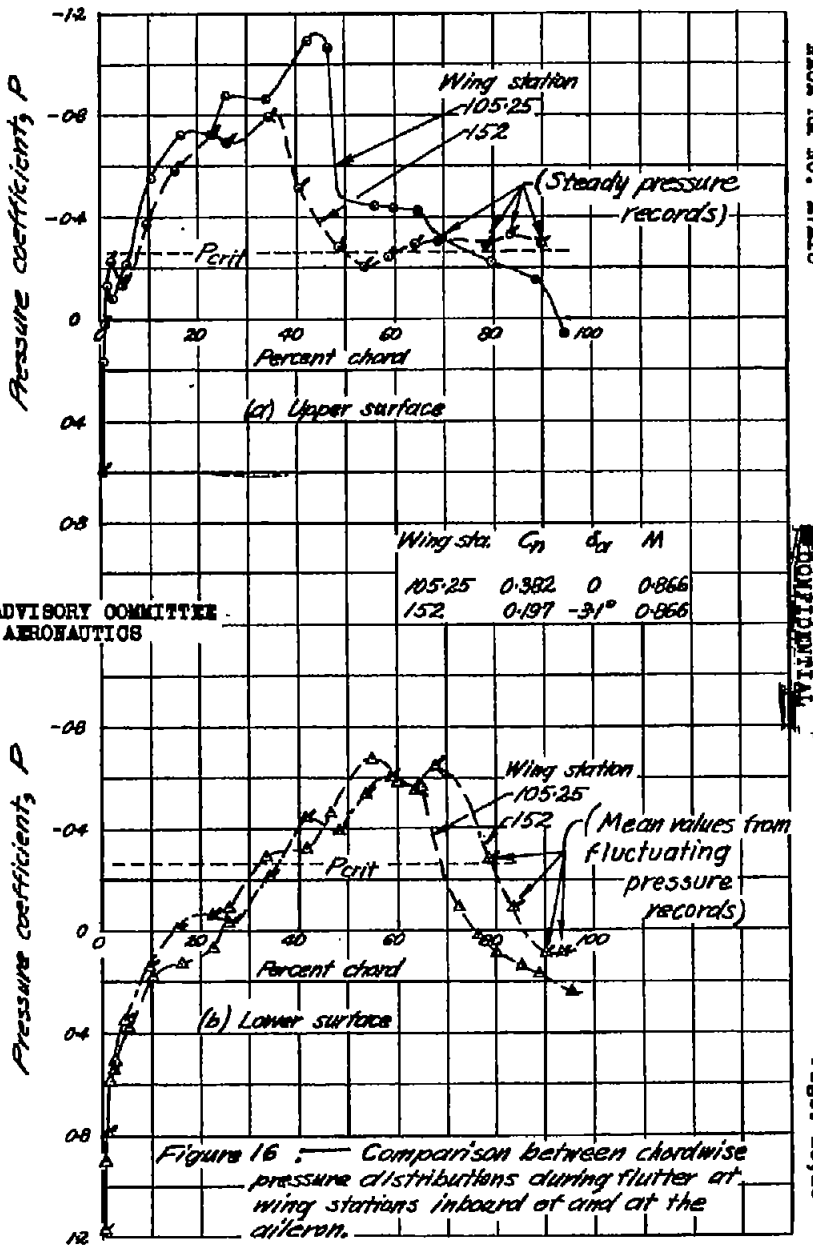

Figure 16. — Comparison between chordwise pressure distributions during flutter at wing stations inboard of and at the aileron.

CONFIDENTIAL

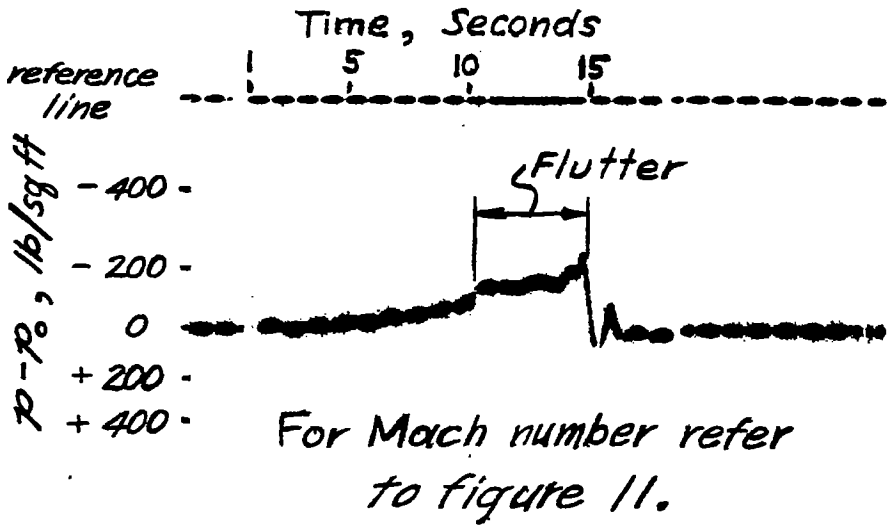

(a) Upper surface at 89.9 percent chord.

NATIONAL ADVISORY COMMITTEE FOR AERONAUTICS

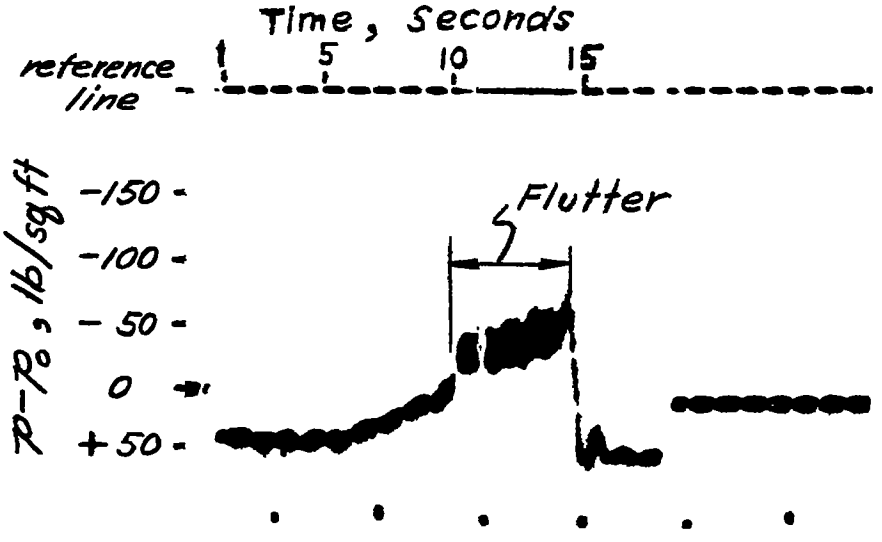

(b) Lower surface at 93.2 percent chord.

Figure 17.- Typical records of pressure orifices on upper and lower surfaces of aileron at wing station 152 during aileron flutter.

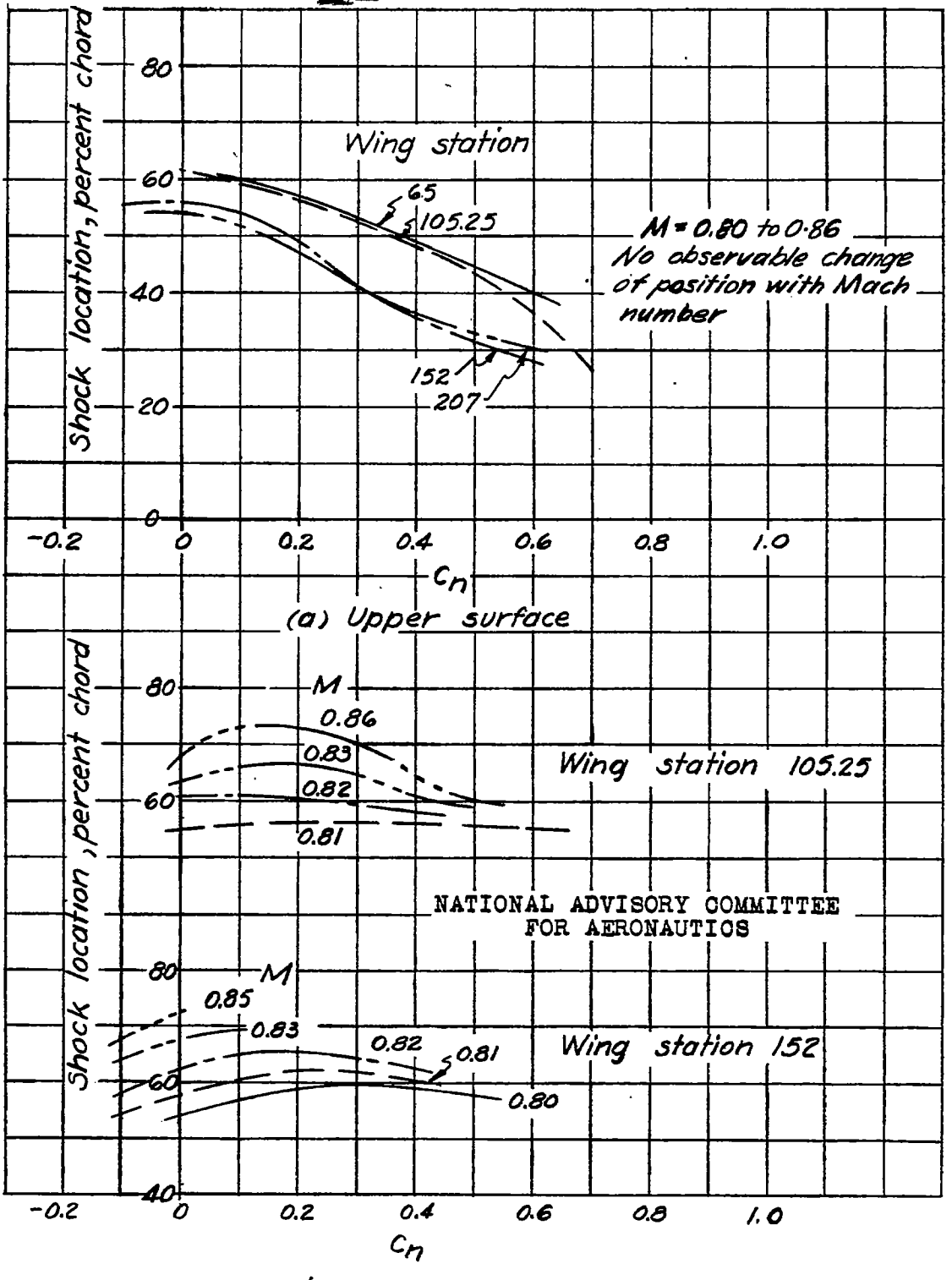

(b) Lower surface

Figure 18 — Chordwise location of the shock wave on the upper and lower surfaces of the wing at supercritical Mach numbers.

CONFIDENTIAL